# Ground-State Simulation Tool for Field-Clocked Three-State Molecular Quantum-dot Cellular Automata (QCA)

Faizal Karim and Konrad Walus
Dept. of Electrical and Computer Engineering
The University of British Columbia
Vancouver, BC, Canada V6T 1Z4
Telephone: (604) 827-3412
Email: {faizalk, konradw}@ece.ubc.ca

***Abstract*—This paper presents the model and implementation of a new numerical simulator within the existing QCADesigner simulation tool capable of treating clocked molecular QCA cells and circuits. The clocking mechanism uses a layer of patterned electrodes to switch the cells by modulating the electrostatic potential energy of the different electronic configurations of the molecular cells. The simulation tool models each QCA cell in the circuit using a three-state Hamiltonian, neglecting the internal degrees of freedom of the molecular cell. We apply the intercellular Hartree approximation (ICHA), treating the interactions between cells classically through expectation values. Using the described numerical simulator, we successfully simulated the majority gate and coplanar crossover circuits.**

## I. Introduction

Molecular quantum-dot cellular automata (QCA) is an emerging nano-scale computing paradigm which utilizes the electrostatic coupling between electronic configurations in neighboring molecules to perform information processing. This computing paradigm was originally introduced by C. S. Lent [1] and has been extended in recent years to devices based on single molecules [2]–[5].

Lent *et al.* proposed an approach to clocking molecular QCA circuits via a field-driven clocking network consisting of a set of submerged electrodes positioned below the layer of cells that generate a traveling vertically-oriented electric field at the level of the QCA molecules [3], [6]–[8] as illustrated in Fig. 1. Here, the signal applied to each of the four electrodes shown in Fig. 1 is shifted by $\phi_i$ as indicated on the electrodes, such that $\phi_1 < \phi_2 < \phi_3 < \phi_4$.

When the applied electric field on the cell, $E_y$, is strongly positive, it will draw the mobile electrons towards the bottom two sites of the cell forcing the cell into the null ("off") state. As the field begins to tend negative, the cell will be in a switching state, partially occupying both the upper and lower sites of the cell. Once the electric field on the cell becomes strongly negative, it will drive the electrons to the upper sites of the cell and force it into one of the active ("on") states. Which of the cell's upper sites are occupied is not determined by the electric field in the $\hat{y}$ direction, but instead by the intercellular interactions between neighboring cells which determine whether a logic "1" or a logic "0" is energetically favorable.

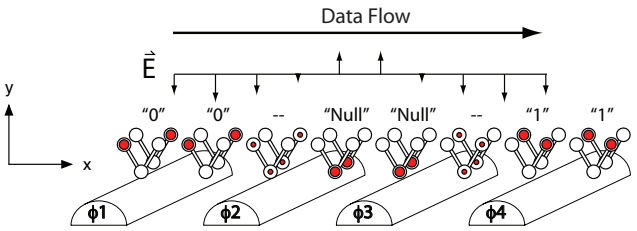


Fig. 1. By applying a phase-shifted sinusoid to each of the electrodes, a forward moving wave can be generated at the level of the cells, forcing cells to switch at the wavefront of this wave. A ground plane located above the cells is not shown in the figure. The sizes of the QCA cells shown here are not to scale with respect to the spacing of the electrodes, and many real cells can be placed between adjacent electrodes.

An open-source numerical simulation tool, QCADesigner [9]–[11] exists for QCA and has been widely applied to the circuit and architectural-level design and exploration of both sequential and combinational circuits [12]–[14]. Currently, QCADesigner assumes that each cell is a simple two-state element and thus realizes the null state using a very delicate coherent superposition - something that can be avoided in the molecular implementation. Furthermore, the tool employs a zone clocking scheme where all cells are grouped into one of four available clocking zones. Each cell in a particular clocking zone is connected to one of the four available phases in the QCA clock such that the height of the tunneling barriers within the cell, and in effect, the transition from an active state to a null state of each cell, is synchronized with the changing clock signal. However, clocking cells in this manner is not likely to be feasible in practice for molecular devices, and thus does not offer a true clocking solution [3].

While others have implemented separate tools capable of modeling a field-driven clocking scheme or the electrostatic coupling between QCA cells, this paper reports on the implementation of an integrated numerical simulator within QCADesigner that has the ability to offer both in the same tool. In doing so, users can access a complete simulation package while taking advantage of the design capability and graphical

user interface of QCADesigner. The flexibility of this tool will allow users to easily design, simulate and characterize a wide-range of three-state QCA circuits.

## II. Model

The simulation tool models each QCA cell in the circuit using a three-state Hamiltonian, where the basis functions are taken to be two fully polarized configurations and the null configuration shown in Fig. 2. This choice of basis is justified by earlier work that demonstrated that the switching behaviour of molecular QCA can be modelled using this reduced basis [15]. Two fixed positive charges are placed underneath the cell to represent the counter-ion and ensure that the system is charge-neutral. The location of the neutralizing charge is determined by the parameter, $d_c$, and is shown to the right in Fig. 2.

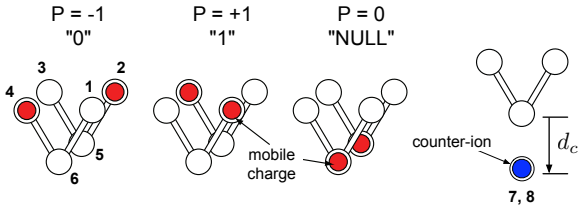


Fig. 2. 3-state QCA cells are composed of "V" shaped molecules grouped in pairs. The location of the counter-ion charge in a 3-dot half cell is shown in the right figure. The numbers next to the individual sites represent the site indexing used throughout the paper.

In order to reduce the computational complexity of solving the many-particle problem exactly for large circuits, the simulation tool applies the inter-cellular Hartree approximation (ICHA) in which individual cells are coupled only through their polarization expectation values. Coherence and correlation are treated exactly within each cell but in the reduced basis described above.

The total charge at each site of a cell and at the location of the counter-ions for the three basis states is

$$Q_+ = \{-e, 0, -e, 0, 0, 0, e, e\}\,, \tag{1}$$

$$Q_- = \{0, -e, 0, -e, 0, 0, e, e\}\,, \tag{2}$$

and

$$Q_{NULL} = \{0, 0, 0, 0, -e, -e, e, e\}\,, \tag{3}$$

where $e$ is the charge of an electron.

Within the following simulation tool, intracellular energies, $E_\kappa^{\text{intra}}$, are computed using simple electrostatics as

$$E_\kappa^{\text{intra}} = \frac{1}{4\pi\epsilon_0}\sum_{i=0}^{6}\sum_{j=i+1}^{7}\frac{Q_\kappa(i)Q_\kappa(j)}{|\vec{r}(i)-\vec{r}(j)|}, \tag{4}$$

where $\kappa = \{+, -, NULL\}$, the indices $i$ and $j$ represent the different sites of the cell, and $Q_\kappa(i)$ is the charge at site, $i$, for a cell in basis state, $\kappa$. These intracellular energies can also be determined using more rigorous *ab initio* quantum chemistry simulations (*i.e.*, CASSCF, etc), and can be fitted to this reduced model as described in [15], [16]. However, for rigid molecules, Equation (4) offers a simple approximation at low computational cost.

The interaction between states in neighbouring cells is pre-calculated based on a fully polarized neighbour. Throughout the simulation, the potential energy, $V_i^{(\text{inter})}$, induced by the intercellular interactions at each of the six sites of the cell is determined according to the following

$$V_i^{(\text{inter})} = \sum_{j\in\mathbf{N}}\sum_{\kappa}|\alpha_{j,\kappa}|^2 V_{i,j}^{\kappa}, \tag{5}$$

where $\alpha_{j,\kappa}$ is the probability amplitude of cell $j$ being in the basis state $\kappa$, and $V_{i,j}^{\kappa}$ is the potential at site $i$ from cell $j$ in the basis state $\kappa$. The probability amplitude is calculated using the time-independent Schrödinger equation. The relevant neighbourhood of cell $i$ is given by the set $\mathbf{N}$ containing all cells which have a distance from cell $i$ less than a user-defined parameter called the *radius of effect*.

At each site, we also add the potential energy from the clocking electrodes, $V_i^{(\text{clock})}$, which is computed by solving Laplace's equation for entire the system. Here, the system consists of electrodes buried in a substrate, a layer of cells, and a ground plane as shown in Fig. 3. The designer can select the medium in which the electrodes and cells exist by independently assigning a relative permittivity to each. The solver begins by dividing the system into a 3-dimensional grid based on the user-defined parameters $\Delta x, \Delta y$, and $\Delta z$. Next, the solver makes an initial guess based on the electrode potentials at $t = 0$, and then solves Laplace's equation at each point in the 3-dimensional grid. The solver repeats this process until the solution converges within a user-specified convergence threshold. Here, the solver assumes Neumann boundary conditions everywhere except for the top and at the electrodes where the Dirichlet boundary condition is used to include the presence of a ground plane and electrode potentials. Continuity of electric flux was enforced at the interface between the substrate and the layer of cells. Fig. 3 shows a cross-section of the system being solved.

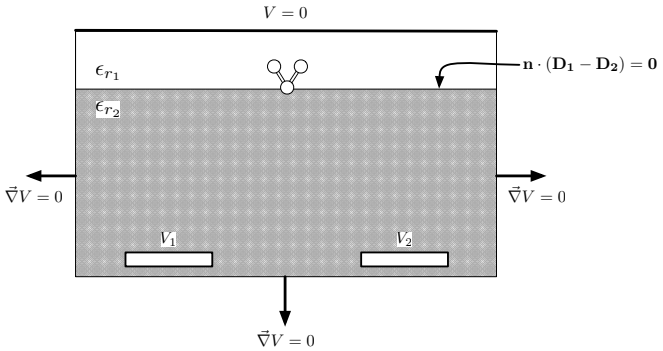


Fig. 3. Cross-sectional view showing the location of the electrodes, ground plane and layer of the QCA cells. The size of the QCA cell is not to scale with respect to the spacing of the electrodes.

The total potential is thus given as

$$V_i = V_i^{(\text{inter})} + V_i^{(\text{clock})}, \tag{6}$$

from which we can determine the electrostatic energy of each of the three basis configurations using

$$E_\kappa = E_\kappa^{\text{intra}} + \sum_{i=0}^{5} V_i Q_\kappa(i). \tag{7}$$

The Hamiltonian for each cell in the reduced basis is thus given as

$$\hat{H} = \begin{bmatrix} E_+ & 0 & -\gamma \\ 0 & E_- & -\gamma \\ -\gamma & -\gamma & E_{NULL} \end{bmatrix}, \tag{8}$$

where $\gamma$ is the tunneling energy between the active states and the null state and depends on the nature of the molecular ligand coupling the redox sites of the molecule (the dots). The off-diagonal zeros between the two active states indicates that no direct coupling exists between the active states, and thus the only tunneling path connecting them is through the null state.

At each time iteration, the time-independant Schrödinger equation is solved, and the resulting wavefunction is used to find the polarization as detailed in [17].

## III. Simulation Results

In this section, we describe the simulation of both the clocking network and two fundamental QCA building blocks using the detailed 3-state engine integrated in QCADesigner. For the former, we used the tool to lay out four $2 \times 10 \times 1$ nm ($w \times l \times h$) electrodes, and plotted the potential profile and field lines at four sequential instances in time. While it is understood that the chosen electrode dimensions may not be practical, the purpose of this work is to demonstrate the function of the described numerical simulator, and as such, electrode dimensions were selected arbitrarily in order to minimize the overall size of the system. A 5 V sinusoid potential was applied to each electrode, with each neighboring electrode phase-shifted by 90° and spaced 7 nm apart. The resulting contour and vector plots are shown Fig. 4. The vertical axis represents the distance between the electrodes and the ground plane (in this case, 10 nm). The relative permittivity of the substrate was chosen to be 12.9 (consistent with gallium arsenide), and the layer of cells was placed 8 nm above the electrodes.

The changing contours and field lines in the four subplots shown in Fig. 4 clearly indicate a traveling wave moving from left to right - allowing for information to be propagated in the same direction.

In a second set of simulations, the functionality of a majority gate and coplanar crossover was investigated. The simulated circuits along with the frequency and phase of each of the clocking electrodes are shown in Fig. 5. Electrode frequencies were chosen based on the expected speed performance of CMOS drivers that would be used to drive clocking electrodes [17], [18]. For both circuits, each of the cells were $1 \times 1 \times 2$ nm ($w \times l \times h$) [8], [16], and were placed 7 nm above the electrodes. The counter-ions were located 5 nm below the null sites of each cell [8], and neighboring cells were spaced 1.5 nm apart. A 5 V sinusoid was applied to each of the

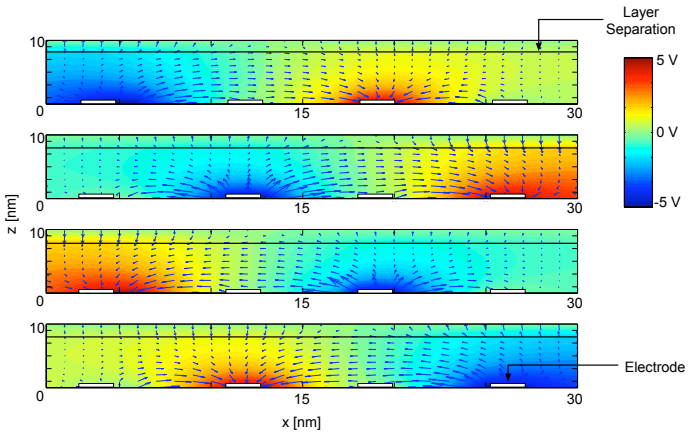


Fig. 4. The potential profile and electric field lines at four sequential instances of time, for four phase-shifted electrodes using QCADesigner. A relative permittivity of 4.2 was used for the substrate.

electrodes, which were placed 10 nm beneath the level of the ground plane. In both cases, the relative permittivity of the substrate was set to 12.9, and the tunneling energy, $\gamma$, was chosen to be 0.1 eV [15]. Circuits were simulated for 70 ps. The electrode potentials used in these simulations were chosen based on the expected switching fields for 1 nm cells placed above a silicon oxide [8].

QCADesigner simulation results for the majority gate and coplanar crossover are shown in Figs. 6 and 7. For the majority gate, a basic four-phase electrode scheme was used to clock the cells. In the coplanar crossover circuit, the clocking scheme proposed by Devadoss *et al.* [19] was used. Here, a central electrode is used to gate the signals in the horizontal and vertical directions in order to allow each signal to propagate alternately without crosstalk. The outputs of each circuit shown in Figs. 6 and 7 clearly verify the correct operation of both building blocks.

## IV. Conclusions

A numerical simulator capable of treating three-state clocked molecular QCA cells and circuits within the QCADesigner tool is introduced. The simulator models each QCA cell in a circuit using a three-state Hamiltonian, with the two fully polarized and null configurations of the cell serving as the basis functions for the cell. The potential energy for each configuration of a cell is computed by summing up the contributions from itself, its neighbors, and the clocking network. The clocking potential was found by solving the 3-dimensional Laplace equation for the entire system. The numerical simulator described in this work has been implemented into QCADesigner and used to successfully simulate a QCA majority gate and coplanar crossover circuit. The simulation tool allows users to easily layout clocking electrodes and cells in a user-defined medium, and provides the user with full control over all electrode and cell dimensions. Users can also adjust the electrode potential, phase and frequency, as well as a cell's tunneling energy, enabling a broad variety of new research studies to be conducted on this technology.

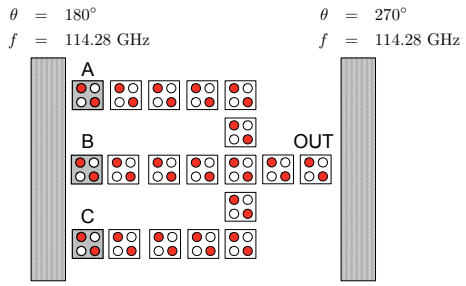


(a) QCA Majority Gate

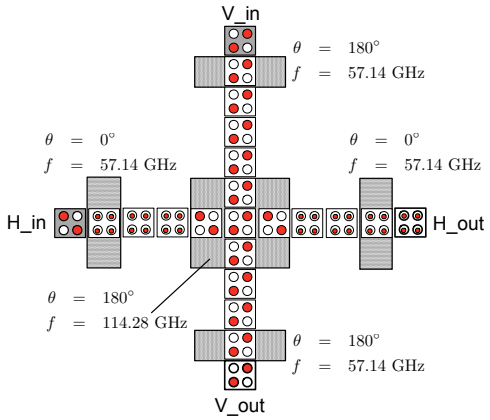


(b) QCA Crossover

Fig. 5. (a) Majority gate layout used in the simulation. (b) Crossover layout used in the simulation.

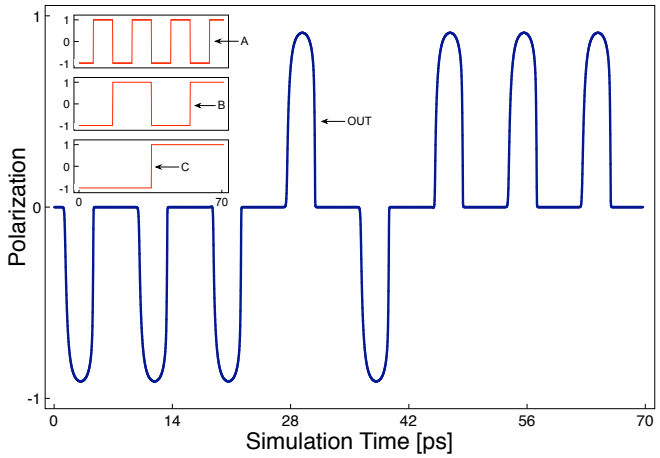


Fig. 6. Simulation results for the majority gate.

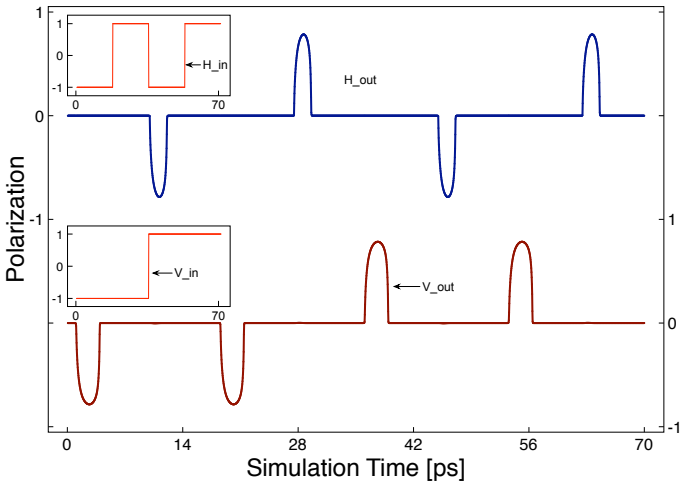


Fig. 7. Simulation results for the coplanar crossover.

## REFERENCES


[1] C. S. Lent, "Quantum cellular automata," *Nanotechnology*, vol. 4, pp. 49–57, 1993.

[2] Y. H. Lu and C. Lent, "Theoretical study of molecular quantum-dot cellular automata," *Journal of Computational Electronics*, vol. 4, pp. 115–118, 2005.

[3] C. S. Lent and B. Isaksen, "Clocked molecular quantum-dot cellular automata," *IEEE Transactions on Electron Devices*, vol. 50, no. 9, pp. 1890–1896, 2003.

[4] Z. Jin, "Fabrication and measurement of molecular quantum cellular automata (QCA) device," Master's thesis, University of Notre Dame, Notre Dame, IN 46556, 2006.

[5] H Qi et. al, "Molecular quantum cellular automata cells. Electric field driven switching of a silicon surface bound array of vertically oriented two-dot molecular quantum cellular automata," *Journal of the American Chemical Society*, vol. 125, no. 49, pp. 15250–15259, 2003.

[6] K. Hennessy and C. S. Lent, "Clocking of molecular quantum-dot cellular automata," *Journal of Vacuum Science & Technology B*, vol. 19, no. 5, pp. 1752–1755, 2001.

[7] E. P. Blair and C. S. Lent, "An architecture for molecular computing using quantum-dot cellular automata," in *Proc. of the Third IEEE Conference on Nanotechnology*, pp. 402–405, 2003.

[8] F. Karim, K. Walus, and A. Ivanov, "Analysis of field-driven clocking for molecular quantum-dot cellular automata based circuits," *J. Comput. Electron.*, vol. 9, pp. 16–30, 2010.

[9] K. Walus and G. A. Jullien, "Design tools for an emerging SoC technology: quantum-dot cellular automata," *Proc. IEEE*, vol. 94, pp. 1225–1244, June 2006.

[10] K. Walus, T. Dysart, G. A. Jullien, and R. A. Budiman, "QCADesigner: A rapid design and simulation tool for quantum-dot cellular automata," *IEEE Trans. Nano.*, vol. 3, pp. 26–31, March 2004.

[11] K. Walus and G. Schulhof, "QCADesigner Homepage," *[Online] http://www.qcadesigner.ca/*, 2001.

[12] K. Walus, M. Mazur, G. Schulhof, and G. A. Jullien, "Simple 4-bit processor based on quantum-dot cellular automata (QCA)," in *Proc. of Application Specific Architectures, and Processors Conference*, pp. 288–293, July 2005.

[13] K. Walus, G. Schulhof, R. Zhang, W. Wang, and G. A. Jullien, "Circuit design based on majority gates for applications with quantum-dot cellular automata," in *Proc. of IEEE Asilomar Conference on Signals, Systems, and Computers*, November 2004.

[14] K. Walus, G. Schulhof, and G. A. Jullien, "High level exploration of quantum-dot cellular automata (QCA)," in *Proc. of IEEE Asilomar Conference on Signals, Systems, and Computers*, November 2004.

[15] Y. H. Lu and C. S. Lent, "A metric for characterizing the bistability of molecular quantum-dot cellular automata," *Nanotechnology*, vol. 19, no. 15, pp. –, 2008.

[16] Y. Lu, M. Liu, and C. Lent, "Molecular quantum-dot cellular automata: From molecular structure to circuit dynamics," *Journal of Applied Physics*, vol. 102, no. 3, pp. 034311–7, 2007.

[17] J. Timler and C. S. Lent, "Maxwell's demon and quantum-dot cellular automata," *Journal of Applied Physics*, vol. 94, no. 2, pp. 1050–1060, 2003.

[18] K. Walus, F. Karim, and A. Ivanov, "Architecture for an external input into a molecular QCA circuit," *J. Comput. Electron.*, vol. 8, pp. 35–42, 2009.

[19] R. Devadoss, K. Paul, and M. Balakrishnan, "Coplanar QCA crossovers," *Electronic Letters*, vol. 45, pp. 1234–1235, November 2010.